

LETTER OPEN



MOLECULAR TARGETS FOR THERAPY

PVR (CD155) epigenetic status mediates immunotherapy response in multiple myeloma

Laura Martínez-Verbo¹, Yoana Veselinova¹, Pere Llinàs-Arias¹, Carlos A. García-Prieto^{1,2}, Aleix Noguera-Castells¹, Miguel L. Pato¹, Alberto Bueno-Costa¹, Ignacio Campillo-Marcos^{1,3}, Lorea Villanueva¹, Aina Oliver-Caldes^{4,5}, Oriol Cardus^{4,5}, Sergi V. Salsench^{4,5}, Almudena García-Ortiz^{6,7}, Antonio Valeri^{6,7}, Elizabeth A. Rojas⁸, Naroa Barrena⁹, Norma C. Gutiérrez^{5,8}, Felipe Prósper^{3,10,11}, Xabier Agirre^{3,10,12}, Carlos Fernández de Larrea^{4,5}, Joaquín Martínez-López^{6,7}, Gerardo Ferrer^{1,3,13}✉ and Manel Esteller^{1,3,14,15}✉

© The Author(s) 2024

Leukemia (2024) 38:2722–2726; <https://doi.org/10.1038/s41375-024-02419-z>

TO THE EDITOR:

The immune system is tightly regulated but plastic in humans. It has several lines of control, and its imbalance has severe consequences for our health. Epigenetics encompasses heritable biochemical changes of the chromatin that do not affect the DNA sequence [1]. Epigenetics is constituted of various levels of control, from structural changes (such as 3D chromatin arrangement) to small biochemical changes (such as DNA methylation) which affect gene expression¹. In the context of immunity, epigenetics has been described to control important events for the system, such as cytotoxic cell activation or exhaustion [2]. Cytotoxic cell activation is critical for tumor clearance. To activate cytotoxicity, several interactions need to occur between the target cell and the immune cell. This group of interactions are commonly known as immune checkpoint (IC) events and determine the outcome of the synapse [3]. IC signals can be co-stimulatory or co-inhibitory, and depending on the amount of signals the immune cells receive, they will determine if the system activates or not. Several rounds of inhibitory signals may induce a senescent state or exhaustion phenotype on the cytotoxic cells [3]. One of these inhibitory markers is the poliovirus receptor (PVR, also known as CD155), which interacts mainly with the T cell immunoreceptor with Ig and ITIM domains (TIGIT) in cytotoxic cells [4]. Tumor cells can use DNA methylation to regulate inhibition of co-stimulatory or overexpression of co-inhibitory markers [3]. Hematological malignancies present aberrant promoter methylation in several immune checkpoint genes and this dysregulation supports their tumorigenesis [5–7]. Multiple myeloma (MM) is a hematological malignancy characterized by the abnormal accumulation of

plasma cells in the bone marrow. MM is notorious for its incurable nature and tendency for relapse, often becoming refractory to treatment [8]. This poses significant challenges, highlighting the urgent need for innovative therapies to enhance the prognosis of affected patients. This work aims to elucidate the epigenetic regulation in PVR, an immune checkpoint marker, and its relation to cytotoxic activation and immunotherapy sensitivity in the context of MM cells.

Distinct expression levels of PVR in primary samples from multiple myeloma (MM) patients [9] suggest that gene expression deregulation could be mediated by alterations in regulatory mechanisms, ranging from epigenetic changes to post-transcriptional modifications. By focusing on DNA methylation, we first observed PVR promoter hypermethylation in a CpG island at the 5′-end of the transcription start site in 14.6% (15 of 104) of primary MM samples available at the European Genome-phenome Archive (EGA) (accession number EGAS00001000841) [10] (see Supplementary Fig. S1). Pyrosequencing analyses (Supplementary Methods) validated the presence of PVR hypermethylation in 2 of 7 additional primary MM samples (Supplementary Table S1). Then, using a comprehensive DNA methylation microarray platform [11] (Supplementary Methods), we observed promoter hypermethylation in a similar 15.4% (2 of 13) of MM cell lines (Fig. 1A). The studied CpG island was found unmethylated in B-Plasma cells (CD138+) from three healthy donors (Fig. 1A), suggesting that the gain of methylation was a cancer-specific event. The CpG island methylation status of the hypermethylated MM cell lines (AMO1 and KMS-12-BM) and of three unmethylated ones (RPMI-8226, JLN-3 and EJM) was further validated by bisulfite genomic

¹Cancer Epigenetics Group, Josep Carreras Leukaemia Research Institute (IJC), Badalona, Spain. ²Barcelona Supercomputing Center (BSC), Barcelona, Spain. ³Centro de Investigación Biomédica en Red Cáncer (CIBERONC), Madrid, Spain. ⁴Department of Hematology, Hospital Clínic de Barcelona, University of Barcelona, Barcelona, Spain. ⁵Institut d'Investigacions Biomèdiques August Pi i Sunyer (IDIBAPS), Barcelona, Spain. ⁶Department of Hematology, Hospital Universitario 12 de Octubre-Universidad Complutense, Instituto de Investigación Sanitaria Hospital 12 de Octubre (imas12), Madrid, Spain. ⁷Hospital Universitario 12 de Octubre-Centro Nacional de Investigaciones Oncológicas (H12O-CNIO). Haematological Malignancies Clinical Research Unit, Spanish National Cancer Research Centre, Madrid, Spain. ⁸Department of Hematology, University Hospital of Salamanca, IBSAL, Cancer Research Center-IBMCC (USAL-CSIC), Salamanca, Spain. ⁹Universidad de Navarra, Tecnun Escuela de Ingeniería, San Sebastián, Spain. ¹⁰Centro de Investigación Médica Aplicada (CIMA), Instituto de Investigación Sanitaria de Navarra (IDISNA), Pamplona, Spain. ¹¹Servicio de Hematología y Terapia Celular, Clínica Universidad de Navarra (CUN), Pamplona, Spain. ¹²Cancer Centre Clínica Universidad de Navarra (CCUN), Pamplona, Spain. ¹³Feinstein Institutes for Medical Research, Northwell Health, Manhasset, USA. ¹⁴Institució Catalana de Recerca i Estudis Avançats (ICREA), Barcelona, Spain. ¹⁵Physiological Sciences Department, School of Medicine and Health Sciences, University of Barcelona (UB), Barcelona, Spain. ✉email: gferrer@carrerasresearch.org; mesteller@carrerasresearch.org

Received: 10 May 2024 Revised: 15 September 2024 Accepted: 18 September 2024

Published online: 24 September 2024

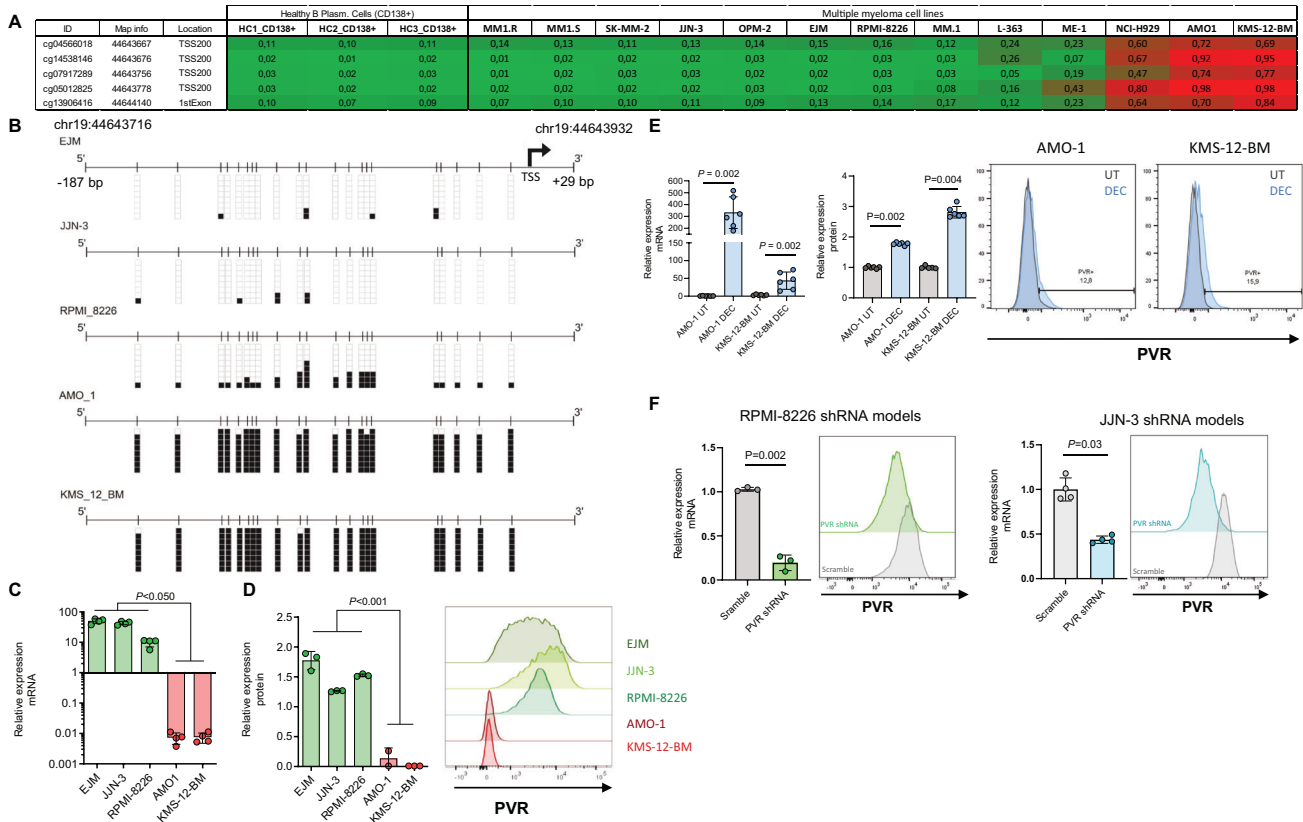


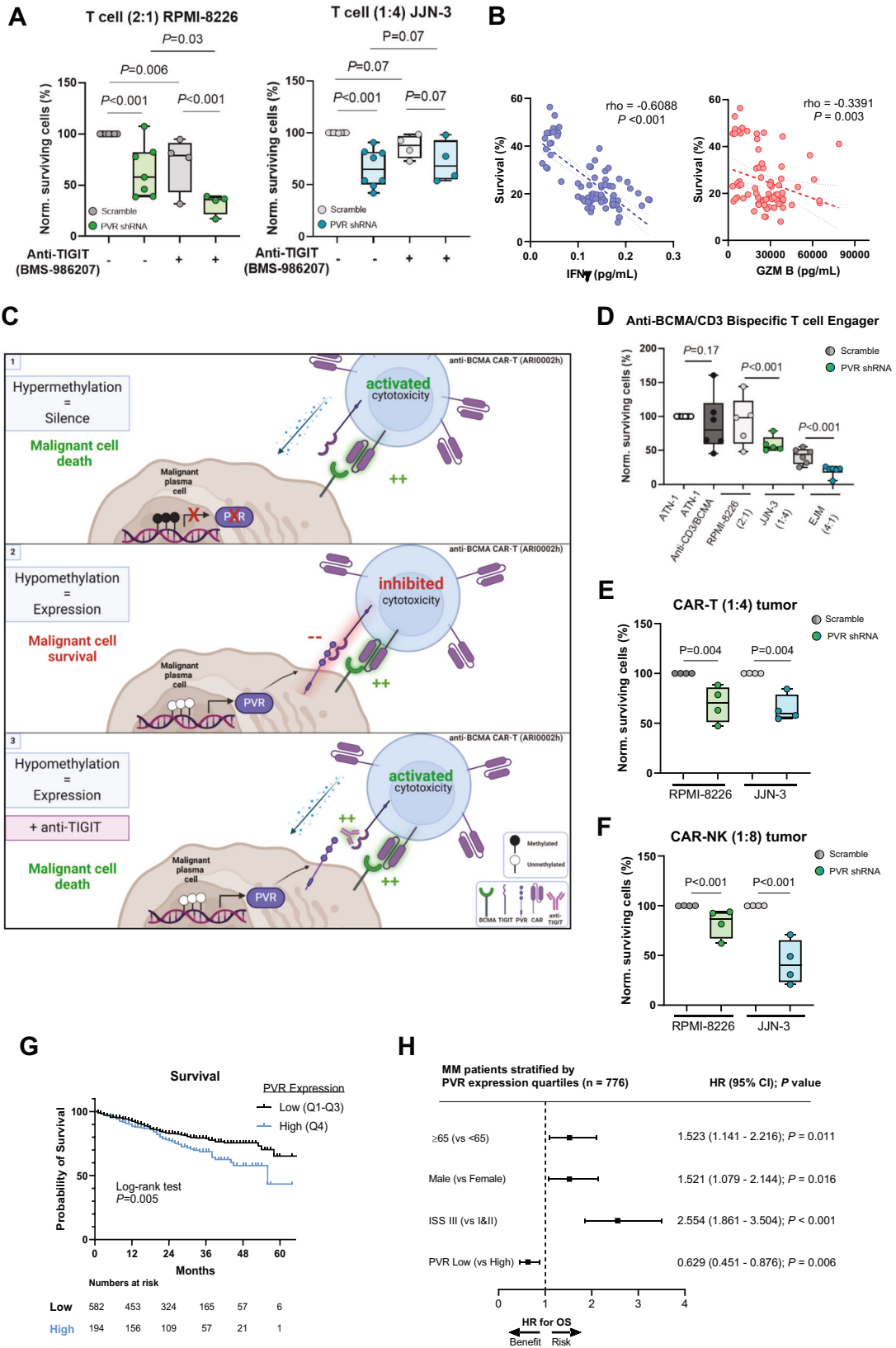
Fig. 1 Epigenetic characterization of PVR shows the correlation between promoter DNA methylation and expression. **A** DNA methylation profile of the PVR promoter CpG island analyzed by the Infinium EPIC DNA methylation array. Single CpG absolute methylation *B*-values are shown (0 to 1). Red, methylated; Green, unmethylated. Thirteen cell lines from multiple myeloma are shown in the figure together with three samples from normal plasmatic B-cells. **B** Bisulfite genomic sequencing of PVR promoter CpG island in multiple myeloma cell lines. CpG dinucleotides are represented as short vertical lines; the TSS is indicated with a black arrow. Single clones are shown for each sample. Black squares represent methylated CpG dinucleotides, whereas white squares denote unmethylated positions. **C, D** PVR expression levels in multiple myeloma cell lines determined by qRT-PCR and flow cytometry protein quantification. The bar plots represent the mean and SD of at least three biological replicates. The results were compared using One-way ANOVA. Representative flow cytometry histograms of PVR are shown for each cell line. **E** Recovery of PVR transcript and PVR protein expression after 1 μ M DEC treatment for 120 h. The graphics represent the mean and SD of at least three biological replicates. The results were compared using unpaired two-tailed Student's *t* test. Representative flow cytometry histograms show the recovery at protein level in AMO-1 and KMS-12-BM cell line. The number indicates the percentages of positive cells for PVR. **F** Efficient shRNA-mediated depletion of PVR at transcript level determined by qRT-PCR and flow cytometry in the unmethylated cell lines RPMI-8226 and JJN-3 from multiple myeloma. The graph represents the mean and SD of at least three biological replicates from three different shRNA models. The results were compared using unpaired two-tailed Student's *t* test.

sequencing of multiple clones (Fig. 1B) (Supplementary Methods). Most importantly, we observed by quantitative RT-PCR (Fig. 1C) and flow cytometry (Fig. 1D) (Supplementary Methods) that both at the RNA and protein levels, respectively, the presence of CpG island hypermethylation was associated with the loss of PVR expression. The link between DNA methylation and transcriptional silencing was further strengthened using the DNA methylation inhibitor 5-aza-2'-deoxycytidine (DEC) that restored PVR expression in the hypermethylated MM cell lines (Fig. 1E).

To study the role of PVR expression levels in engaging immune response in MM, we successfully created stable models of PVR depletion by shRNA interference in the expressing and unmethylated MM cell lines RPMI-8226 and JJN-3 (Fig. 1F) (Supplementary Methods). To assess the effect of PVR downregulation in T cell cytotoxicity, we developed a co-culture system where T cells from healthy individuals were cultured for 48 h in the presence of the MM cell line models (Supplementary Methods). We considered biological variability by performing all the experiments with T cells from at least four different donors. We observed that shRNA-mediated depletion of PVR induced an increase in the cytotoxicity of T cells on both MM cell lines in comparison with shRNA-scrambled cells (Fig. 2A). To define further the mechanisms by

which PVR downregulation increases T cell cytotoxicity, we performed the same co-culture experiments in the presence of the anti-TIGIT antibody BMS-986207, since PVR is a ligand of this T cell immunoreceptor that restrains immune activation [4]. We found that the increased susceptibility to T cell cytotoxicity mediated by PVR knockdown can be augmented in some cases using the anti-TIGIT antibody (Fig. 2A). The enhancement of cell death was accompanied with the augment of interferon gamma and granzyme b (Fig. 2B).

The above results prompted us to assess the impact of PVR expression levels on different immunotherapy approaches designed against MM: an anti-CD3/BCMA bispecific T cell engager, an anti-BCMA CAR-T and an anti-BCMA CAR-NK (Fig. 2C). For the initial strategy, following the demonstration that the antibody had no effect on a T-ALL cell line (that does not express BCMA), we found that the shRNA-mediated depletion of PVR in MM cells increased T cell toxicity upon the used of the bispecific antibody (Fig. 2D). For adoptive cell therapies, we used ARI0002h, an academic second-generation humanized 4-1BB-based CAR transduced on autologous T, for which promising results in MM have been recently published [12]. Since one of the main suspects for CAR-T treatment failure is T cell exhaustion [13], we evaluated how



our MM models for PVR levels related to the presence of CAR-T cells. We observed overall an enhanced cytotoxicity of PVR-depleted MM cells upon exposure to CAR-T cells (Fig. 2E). Finally, we explored the potential use of CAR-NK cells in our models, since

they lack several of the complications associated with CAR-Ts (i.e. ICANS or CRS [14, 15]) and share some regulatory mechanisms with T cells, including the expression of TIGIT [15]. In these experiments, for the two MM cell lines, we found that anti-BCMA

Fig. 2 Depletion of PVR in the multiple myeloma cell lines, functional characterization of models, co-culture experiments and clinical impact. **A** Percentage of MM surviving cells determined by Annexin V incorporation in co-culture assay for 48 h between healthy donor T cells and PVR-depleted cells. The ratios to control cells were represented as surviving portion of cells. **B** Representative pro-inflammatory cytokines (IFN γ and GZMB) levels measured in the supernatant (at 48 h) of the co-culture systems with J2N-3 determined by ELISA assay. Spearman correlation was used to measure statistical significance. Dotted lines represent 95% confidence interval. **C** Graphical representation of the influence of PVR in the interaction between malignant B plasmatic cells and different immunotherapy approaches. **D** Percentage of surviving cells determined by Annexin V incorporation in co-culture assay for 48 h between healthy donor T cells and PVR-depleted cells in the presence of the Bispecific T cell Engager at 10 ng/ml. ATN-1 is a T-ALL not expressing one of the targets for the Bispecific T cell Engager. **E** Percentage of MM surviving cells determined by Annexin V incorporation in co-culture assay for 24 h between PVR-depleted cells and anti-BCMA CAR-T at 1:4 ratio. **F** Percentage of J2N-3 and RPMI-8226 surviving cells determined by Annexin V incorporation in co-culture assay for 24 h between PVR-depleted and anti-BCMA CAR-NK at 1:8 ratio. Statistics: Each dot represents the mean of each of the donors with at least three biological replicates from four different healthy donors. The results were compared using non-parametric paired Wilcoxon test. **G** Kaplan–Meyer survival curves for $n = 756$ patients of MM dividing by expression levels of PVR. **H** Forest plot of overall survival (OS) in subgroups stratified by clinical factors and PVR expression quartile.

CAR-NK cells showed enhanced cell cytotoxicity in the context of shRNA-mediated depletion of PVR (Fig. 2F). Incorporating anti-TIGIT antibody in all previous experiments, increased scrambled MM cells (unmethylated and expressing PVR) susceptibility to the different immunotherapy strategies (Supplementary Fig. S2).

Finally, we analyzed the highly informative CoMMpass project, which includes 776 cases of newly diagnosed multiple myeloma (MM) [8]. In this dataset, we examined the expression of the PVR transcript in CD138+ cells. Notably, we found that low levels of PVR mRNA were associated with extended overall survival compared to MM patients with high transcript levels (Log-rank test: $P = 0.005$, HR = 0.596; 95% CI = 0.415–0.854) (Fig. 2G). Remarkably, multivariate Cox regression analysis indicated that lower PVR expression was an independent predictor of longer overall survival (HR = 0.629; 95% CI = 0.451–0.876; $P = 0.006$) when adjusted for available clinical parameters (age, gender, and the Multiple Myeloma International Staging System, ISS) (Fig. 2H). Furthermore, in a subset of patients with cytogenetic information, we observed that high PVR expression was associated with high-risk alterations such as t(4;14), gain of 1q21, del(13q14), and del(1p22). Conversely, lower PVR expression was linked to lower-risk alterations such as t(11;14) and t(8;14) (Supplementary Fig. S3).

Altogether, these results suggest that better outcomes in multiple myeloma (MM) cases with low PVR might be associated with enhanced immune system engagement. Consequently, targeting PVR may represent a promising therapeutic strategy to improve clinical outcomes in MM. However, immune checkpoint inhibitors used as monotherapy for MM have not proven very effective and do not show the same promise as bispecific antibodies and cellular therapies for relapsed disease. Nonetheless, there is potential in combination therapies. Cytotoxic cell exhaustion remains a predictor of response to immunotherapy, and our in vitro results support the idea that the direct targeting of PVR on malignant cells can enhance the efficacy of bispecific antibodies and adoptive cell therapies in MM patients.

REFERENCES

- Peixoto P, Cartron PF, Serandour AA, Hervouet E. From 1957 to nowadays: a brief history of epigenetics. *Int J Mol Sci.* 2020;21:1–18.
- Villanueva L, Álvarez-Erriço D, Esteller M. The contribution of epigenetics to cancer immunotherapy. *Trends Immunol.* 2020;41:676–91.
- Xia Y, Medeiros LJ, Young KH. Immune checkpoint blockade: releasing the brake towards hematological malignancies. *Blood Rev.* 2016;30:189–200.
- Kučan Brlić P, Lenac Roviš T, Cinamon G, Tsukerman P, Mandelboim O, Jonjić S. Targeting PVR (CD155) and its receptors in anti-tumor therapy. *Cell Mol Immunol.* 2019;16:51–63.
- Muylaert C, Van Hemelrijck LA, Maes A, De Veirman K, Menu E, Vanderkerken K, et al. Aberrant DNA methylation in multiple myeloma: a major obstacle or an opportunity? *Front Oncol.* 2022;12:1–24.
- Avella Patino DM, Radhakrishnan V, Suvilesh KN, Manjunath Y, Li G, Kimchi ET, et al. Epigenetic regulation of cancer immune cells. *Semin Cancer Biol.* 2022;33:377–83.
- Keshari S, Barrodia P, Singh AK. Epigenetic perspective of immunotherapy for cancers. *Cells.* 2023;12:1–20.

- The Multiple Myeloma Research Foundation (MMRF). CoMMpass Project. <https://gdc.cancer.gov/about-gdc/contributed-genomic-data-cancer-research/foundation-medicine/multiple-myeloma-research-foundation-mmrf>. Accessed: September 2022.
- Lozano E, Mena MP, Díaz T, Martín-Antonio B, Leon S, Rodríguez-Lobato LG, et al. Nectin-2 expression on malignant plasma cells is associated with better response to TIGIT blockade in multiple myeloma. *Clin Cancer Res.* 2020;26:4688–98.
- Duran-Ferrer M, Clot G, Nadeu F, Beekman R, Baumann T, Nordlund J, et al. The proliferative history shapes the DNA methylome of B-cell tumors and predicts clinical outcome. *Nat Cancer.* 2020;1:1066–81.
- Moran S, Arribas C, Esteller M. Validation of a DNA methylation microarray for 850,000 CpG sites of the human genome enriched in enhancer sequences. *Epi-genomics.* 2016;8:389–99.
- Oliver-Caldés A, González-Calle V, Cabañas V, Español-Rego M, Rodríguez-Otero P, Reguera J, et al. Fractionated initial infusion and booster dose of ARI0002h, a humanised, BCMA-directed CAR T-cell therapy, for patients with relapsed or refractory multiple myeloma (CARTBCMA-HCB-01): a single-arm, multicentre, academic pilot study. *Lancet Oncol.* 2023;24:913–24.
- Mishra AK, Schmidt TM, Martell EB, Chen AS, Dogru RE, Hematti P, et al. PD1+TIGIT+2B4+KLRG1+ cells might underlie T cell dysfunction in patients treated with BCMA-directed chimeric antigen receptor T cell therapy. *Transpl Cell Ther.* 2024;30:191–202.
- Leivas A, Valeri A, Córdoba L, García-Ortiz A, Ortiz A, Sánchez-Vega L, et al. NKG2D-CAR-transduced natural killer cells efficiently target multiple myeloma. *Blood Cancer J.* 2021;11:1–11.
- Valeri A, García-Ortiz A, Castellano E, Córdoba L, Maroto-Martín E, Encinas J, et al. Overcoming tumor resistance mechanisms in CAR-NK cell therapy. *Front Immunol.* 2022;13:1–28.

ACKNOWLEDGEMENTS

We thank CERCA Programme / Generalitat de Catalunya for institutional support. The Secretariat for Universities and Research of the Ministry of Business and Knowledge of the Government of Catalonia has provided funding to ME (2017 SGR1080 and 2021 SGR01494). ME has also received funding from the Spanish Ministry of Science and Innovation MCIN/AEI/10.13039/501100011033/EDRF 'A way to make Europe' (RTI2018-094049-B-I00 and PID2021-125282OB-I00), Cellex Foundation (CEL007) and "la Caixa" Foundation (LCF/PR/HR22/00732). LMV is a fellow of the Spanish Ministry of Science and Innovation grant under FPI contract no. PRE2019-089958. AOC received funding from the resident grant Ajut Clínic-La Pedrera 2019, granted by Hospital Clínic de Barcelona. CFL has received funding by grants from Asociación Española Contra el Cáncer (AECC) LABAE21971FERN, the Instituto de Salud Carlos III (ISCIII) and co-funded by the European Union (FIS P122/00647 and ICI19/00025), and 2021SGR01292 (AGAUR; Generalitat de Catalunya). GF is recipient of Ayuda Investigador AECC 2023 (INVE234765FERR), Fundación Científica AECC. We thank Bristol Myer Squibb for providing BMS-986207 anti-TIGIT Neutralizing Antibody and Genomics Unit of Josep Carreras Leukaemia Research Institute for their help and the advice provided.

AUTHOR CONTRIBUTIONS

Contribution: LMV, PLA, LV, GF and ME conceived and designed the study; LMV performed all experiments; YV, CAGP, ANC and DP analyzed in silico data; YV and ML performed pyrosequencing PCR; AB, IC, NB, FP and XA processed and analyzed primary data; AOC, OC, SVS, AGO, AV, EAR, NCG, CFL, JML and GF provided CAR constructs and primary samples; All authors provided scientific advice and result discussion; and LMV, GF and ME wrote the manuscript with contributions and approval from all authors.

COMPETING INTERESTS

The authors declare that the research was conducted in the absence of any commercial or financial relationships that could be considered as a potential conflict of interest.

ADDITIONAL INFORMATION

Supplementary information The online version contains supplementary material available at <https://doi.org/10.1038/s41375-024-02419-z>.

Correspondence and requests for materials should be addressed to Gerardo Ferrer or Manel Esteller.

Reprints and permission information is available at <http://www.nature.com/reprints>

Publisher's note Springer Nature remains neutral with regard to jurisdictional claims in published maps and institutional affiliations.



Open Access This article is licensed under a Creative Commons Attribution-NonCommercial-NoDerivatives 4.0 International License, which permits any non-commercial use, sharing, distribution and reproduction in any medium or format, as long as you give appropriate credit to the original author(s) and the source, provide a link to the Creative Commons licence, and indicate if you modified the licensed material. You do not have permission under this licence to share adapted material derived from this article or parts of it. The images or other third party material in this article are included in the article's Creative Commons licence, unless indicated otherwise in a credit line to the material. If material is not included in the article's Creative Commons licence and your intended use is not permitted by statutory regulation or exceeds the permitted use, you will need to obtain permission directly from the copyright holder. To view a copy of this licence, visit <http://creativecommons.org/licenses/by-nc-nd/4.0/>.

© The Author(s) 2024